

## The Influence of Stabilizing Impurities and Annealing on the Structure and Mechanical Properties of Partially Stabilized Zirconia

F.O.Milovich<sup>1,\*</sup>, N.Y.Tabachkova<sup>1</sup>, V.T.Bublik<sup>1</sup>, E.E.Lomonova<sup>2</sup>,  
M.A.Borik<sup>2</sup>, A.V.Kulebyakin<sup>2</sup>, V.A.Myzina<sup>2</sup>, V.V.Osiko<sup>2</sup>

<sup>1</sup> National University of Science and Technology "MISIS", 117936 Moscow, Leninsky pr., 4

<sup>2</sup> Prokhorov General Physics Institute, Russian Academy of Sciences, 119991, Moscow, Vavilov Str., 38

(Received 4 July 2012; published online 18 August 2012)

The phase composition and evolution of the twin structure of PSZ crystals, depending of the concentration stabilizing impurities have been investigated by X-ray diffraction and transmission electron microscopy. The measurements of hardness and fracture toughness by microindentation have been carried out. In work is shown that the high mechanical characteristics of PSZ crystals are related to features of their phase composition and structure, namely the degree of tetragonality the phase and the presence of domains ranging in size from tens to hundreds of nanometers.

**Keywords:** Partially stabilized zirconia, transmission electron microscopy, X-ray diffraction, materials of high strength and durability, skull melting technique in a cold crucible.

PACS numbers: 61.10.Nz, 62.20. – x, 68.37.Lp

### 1. INTRODUCTION

The partially stabilized zirconia crystals (PSZ), at the expense of its unique structure, have high tribological characteristics. Their properties allow using of the material where strength is required when sliding and friction in conjunction with high temperatures, aggressive environments and extreme loads. The combination of properties such as fracture toughness, hardness, wear resistance, low friction coefficients, chemical and biological inertness, makes PSZ crystals are promising materials for the manufacture of durable and super acute medical tool. The high strength of PSZ crystals allows producing tools with sharpness cutting edge to 100 nm for cardiology and neurosurgery, vascular surgery, ophthalmology, etc. [1].

Such properties of PSZ crystals are related to features of their phase composition and structure, namely the presence of nano and micro twin structure [2]. Technological change in the growth conditions and annealing of PSZ crystals affects on the structure and therefore on the mechanical properties of the material. The subject of the investigation is evolution of phase composition and the twin structure, depending on the impurity concentration  $Y_2O_3$ , as well as the identification of influence of the dopant on the microhardness and fracture toughness of PSZ crystals, i.e. establishing connection with the mechanical properties of the structure.

### 2. EXPERIMENTAL

#### 2.1 Materials

PSZ crystals were grown by directional solidification in a cold crucible (induction skull melting technique). The growth of PSZ crystals was carried out in the range of compositions  $ZrO_2 - Y_2O_3$  (2.8, 3.0, 3.2, 3.7, 4.0 mol. %). The dimensions of grown crystals were: a cross-section of 10 to 50 mm, height from 70 to 100 mm. The wafers were cut from the crystals, thickness about 300  $\mu$ m, theirs plane was oriented perpendicular to the  $\langle 100 \rangle$  and  $\langle 111 \rangle$  axis of the crystal.

#### 2.2 Instruments

Investigation of phase composition was performed by means of x-ray diffraction Bruker D8. The structure was investigated by transmission electron microscopy using a microscope JEM 2100 at an accelerating voltage of 200 kV. The samples were polished to a thickness of 200  $\mu$ m for preparation to TEM studies. To cut a disc of 3 mm thick was used ultrasonic cutting, and then the hole was formed in the central part of the disc. For further thinning of the samples was used ion etching. The measurements of microhardness and fracture toughness were carried out on Vickers microhardness 402MVD Instron Wolpert Wilson Instruments with a maximum load of up to 2 kg, and Wolpert Hardness Tester 930 with a minimum load of 5 kg on the wafer with the planes, which was cut parallel to the planes (001).

### 3. RESULTS AND DISCUSSION

#### 3.1 Phase analysis

In the diffraction pattern was obtained from a sample, cut out from the crystal along the plane (100). There were reflections - second, fourth and sixth orders from this plane. A more detailed consideration area diffraction pattern of large-angles  $2\theta$  showed that this material has two tetragonal phases belonging to space group symmetry  $R42/mnc$ , as seen in Fig. 1a. The appearance of the diffraction reflections at the same time (006) and (600) is due to twinning, as will be shown below in the study by transmission electron microscopy. The imposition of the splitting of reflections due to the tetragonality and the splitting of the  $K_\alpha$  doublet prevented the analysis of the profile of the diffraction lines. Therefore, an experiment was conducted with the  $K_\beta$  radiation, which confirmed the splitting of the lines and the presence of these two tetragonal phases.

The phase composition of zirconia doped with different concentrations  $Y_2O_3$  by X-ray diffraction showed that all studied samples, independently of the content

\* [filippmilovich@mail.ru](mailto:filippmilovich@mail.ru)

of stabilizing impurities, have two phases of tetragonal zirconia with varying degrees of tetragonality. For a tetragonal phase  $t$  with the ratio  $c/a$  was 1,014-1,015, for the other tetragonal phase  $t'$  ratio  $c/a$  little different from the 1 and amounted to 1,004-1,005. Yttrium-enriched phase of  $t'$  is "nontransformable" in contrast to the  $t$  phase, with a lower content of yttrium, which under the influence of mechanical stress undergoes martensitic transition to the monoclinic form. Increasing the concentration of the stabilizing impurity from 2.8 to 4.0 mol. %  $Y_2O_3$ , leads to a monotonic increase in the quantity weak-tetragonal phase and a decrease in the quantity of "transformed" phase.

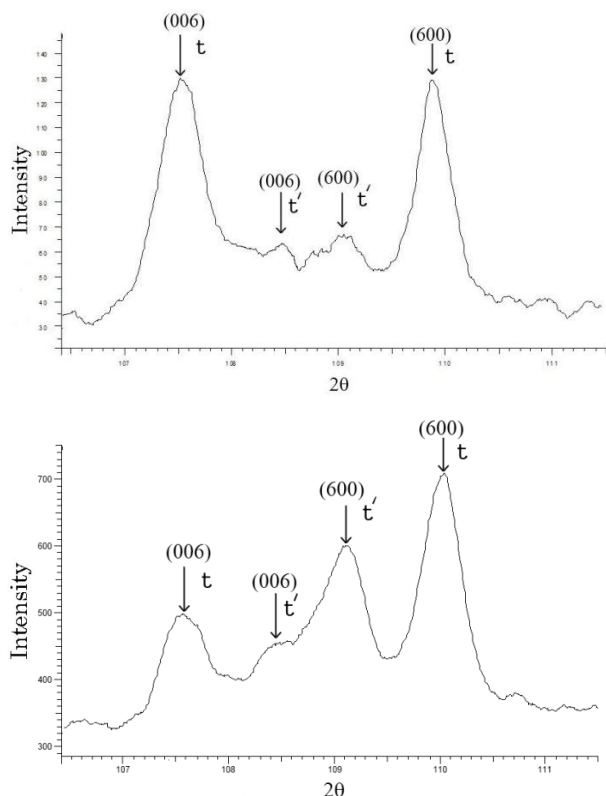


**Fig. 1** – a: X-ray diffraction patterns of the YSZ 2.8 mol. %  $Y_2O_3$ ; b: X-ray diffraction patterns of the YSZ 4.0 mol. %  $Y_2O_3$

### 3.2 Research of structure partially stabilized zirconia crystals

Investigation of the structure of zirconium dioxide in the TEM showed that the appearance electron diffraction patterns, all of the samples were single crystalline. Fig. 2 presents a typical electron diffraction pattern of samples cut out across a  $\langle 111 \rangle$  axis of a crystal. On the electron diffraction, there are reflections of the type  $(110)$  are forbidden in the cubic lattice and allowed in the tetragonal, that confirms the results of x-ray analysis. TEM method is not able to separate the two tetragonal phases, due to their close lattice parameters. All of the samples had a twin domain structure. Fig. 3 is an electron micrograph of microtwins in the  $[100]$ -oriented  $ZrO_2$  2.8 mol %  $Y_2O_3$  sample.

Most of the domains are elongated. The twinning plane of the domains is  $\{110\}$ . Primary twin plates are also twinned, forming a herringbone structure of twin

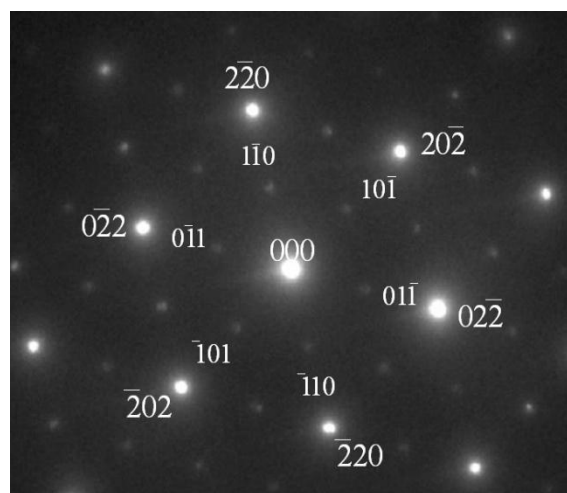


**Fig. 2** – Selected area diffraction pattern of a sample in a  $\langle 111 \rangle$  direction with reflections from  $(110)$ , which corresponding to the tetragonal phase

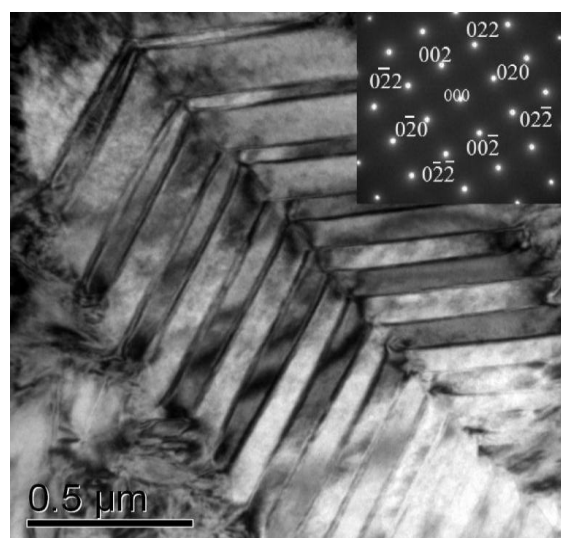


**Fig. 3** – Bright-field image of twin domains in the  $ZrO_2$  2.8 mol. %  $Y_2O_3$  sample

domains. Twinning occurs on planes inclined to the four fold axis  $C$ . Twinning is possible on the  $(101)$  and  $(011)$  planes and impossible on the  $(110)$  plane, parallel to the  $C$  axis. High resolution TEM examination revealed twins on the order of 15 nm in size (Fig. 4). It is reasonable to assume that the twinning process continues as long as there is elastic stress sufficient for twinning. Study of PSZ crystals with different concentrations of the stabilizing impurity showed that increasing in the concentration of  $Y_2O_3$  affect the form and dispersion of the twin domains. At a concentration of  $Y_2O_3$  from 2.8 to 3.2 mol. % twinning first goes in the larger domains, which in turn also twinned.

Observation of twin domains in the high resolution showed that nano-sized twins are found only in samples with concentrations up to 3.2 mol. %  $Y_2O_3$ . At high concentrations, the stabilizing impurity (3.7 – 4 mol. %  $Y_2O_3$ ) hierarchy of twinning is not visible, traces of atomic planes within the domains are not violated. It allows assuming that the twinning occurs at the same time and is localized in small volumes. At the cooling

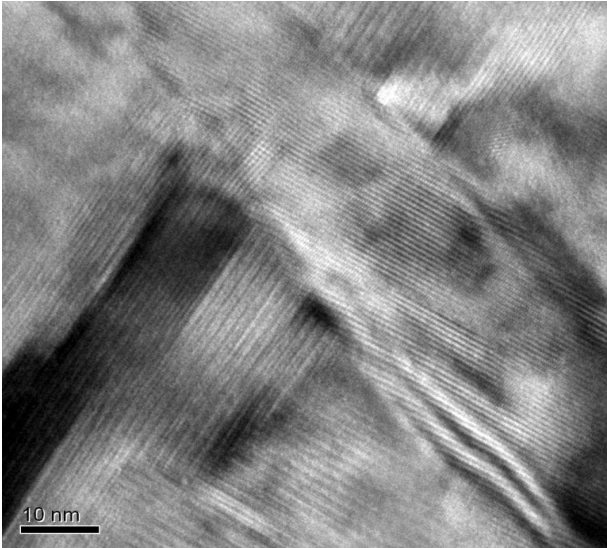


**Fig. 4** – High-resolution TEM image of twin domains in the  $ZrO_2$  2.8 mol. %  $Y_2O_3$  sample

the crystal phase transition from cubic to two-phase region, in accordance with the phase diagram, occurs at lower temperatures, therefore the character of the twinning structure was changing. The relative position of domains in a sample of 3.7 mol. % was different from the other concentrations. Generally domains were arranged perpendicular to each other, as shown in Fig. 5.

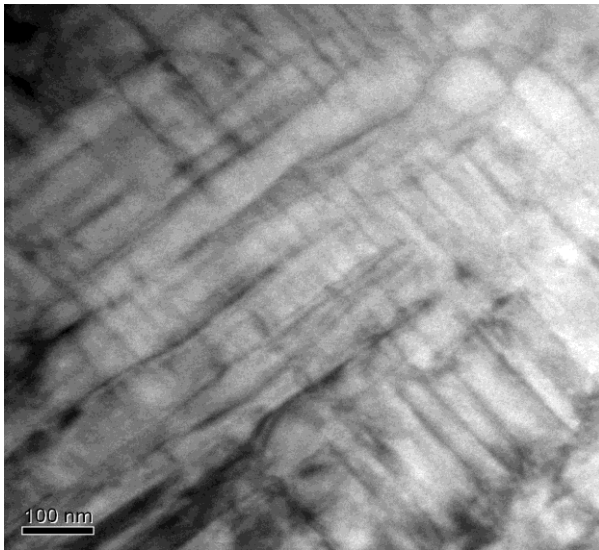


**Fig. 5** – Bright-field image of twin domains in the  $ZrO_2$  3.7 mol. %

With increasing impurity concentration to 4.0 mol. % the morphology of the twins changed, as shown in Fig. 6.

### 3.3 Mechanical properties

For detection of anisotropy in the PSZ crystals, measurements of microhardness and fracture toughness were carried out in different directions, on oriented samples. For this purpose, each sample was oriented on a diffractometer and glued on the plane-parallel substrate, which indicated the direction of the axes. For measuring the microhardness there were chosen loads

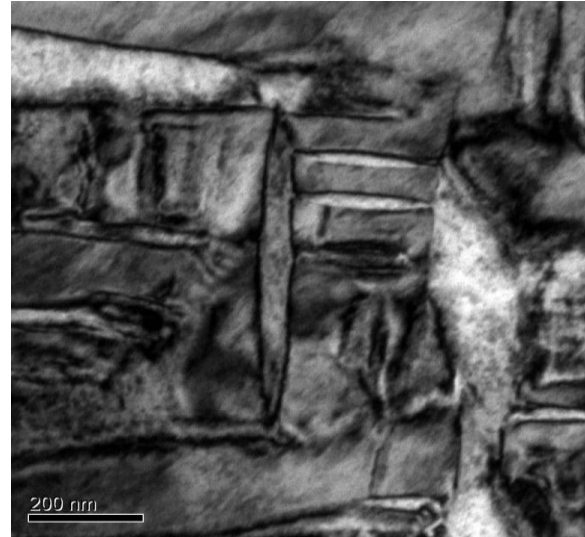


**Fig. 6** – Bright-field images of twin domains in the  $ZrO_2$  4.0 mol. %  $Y_2O_3$  sample

at which the microhardness independent of the load. As microhardness anisotropy was not observed, further measurements for a set of statistics were carried out in one direction. Fracture toughness was determined by the formula:

$$K_{Ic} = 0,035(L/\alpha)^{-1/2} (CE/H)^{2/5} H\alpha^{1/2} C^{-1}, \quad (1.1)$$

where:  $K_{Ic}$  – intensity factor stresses,  $L$  – length of radial cracks,  $\alpha$  – half-width of the printout,  $C$  – Poisson's ratio,  $E$  – Young's modulus,  $H$  – microhardness.

For obtaining dependence fracture toughness on the percentage of  $Y_2O_3$  content, was chosen the total load for all concentrations. For the measurements was chosen load of 10 kg. Fracture toughness, as the microhardness was measured in all directions. In all samples the cracks arose on ends of the diagonals of the indentation, as shown in Fig. 7.

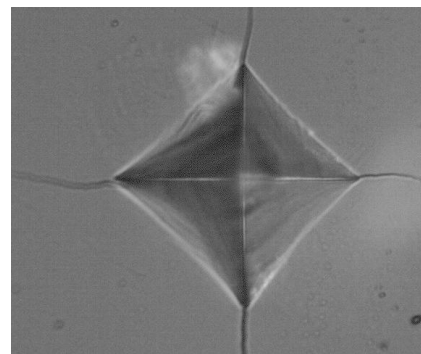


**Fig. 7** – Vickers indentation on the (001) plane of PSZ with cracks are clearly visible

After comparing fracture toughness in all directions, it turned out that the difference lies in the range of values error. Thus, further measurements were performed for a set of statistics in one direction only. The resulting average values of fracture toughness and microhardness with error measurement are presented in Table 1.

**Table 1** – Dependence of microhardness and fracture toughness from the  $Y_2O_3$  concentration

Compositions $Y_2O_3$ , %				
2,8	3,0	3,2	3,7	4,0
The values of microhardness, HV (300 g)				
1410±40	1420±30	1400±20	1420±25	1450±40
The values fracture toughness, $MPa \cdot m^{-1/2}$ (10 kg)				
12±0,6	10±0,6	9±0,6	7±0,6	6±0,6

The table shows that the correlation between the composition and microhardness, within error, is not observed, but it is clear that with increasing concentration of  $Y_2O_3$ , fracture toughness decreases. The sample with the lowest concentration of the stabilizing impurity 2.8 mol. % showed the most resistant to cracking. Good mechanical properties can be associated with a

complex twin structure, while fracture toughness decrease agrees with decrease in the quantity of t phase. The decrease t phase, affects the "transformational" hardening, when the moving microcrack induces martensitic t-m transition, which absorbs the energy of stresses, and eventually stops the microcrack.

## REFERENCE

1. M.A. Borik, E.E. Lomonova, V.V. Osiko, V.A. Myzina, *J. Cryst. Growth* **275**, 2173 (2005).
2. N.Y. Tabachkova, E.E. Lomonova, M.A. Borik, F.O. Milovich, V.T. Bublik, A.V. Kulebyakin, V.A. Myzina, V.V. Osiko, *J. Inorg. Mater.* **48** №2, 158 (2012).